

MOMENTUM OF INERTIA FOR THE ^{240}Pu ALPHA DECAY

M. MIREA

Horia Hulubei National Institute for Physics and Nuclear Engineering,
Department of Teoretical Physics,
Reactorului 30, RO-077125, POB-MG6, Măgurele-Bucharest, Romania

Received August 26, 2014

The momentum of inertia is calculated for the ^{240}Pu alpha decay process within the cranking model. The alpha decay is treated as a superasymmetric fission process within the macroscopic-microscopic model. The microscopic part is based on the Woods-Saxon two center shell model. The moment of inertia exhibits a rapid variation in the vicinity of the ground state of the parent configuration.

Key words: Macroscopic-microscopic model, ^{240}Pu , alpha decay.

PACS: 21.60.Cs.

1. INTRODUCTION

Usually, the alpha decay is treated in the framework of the Gamow model. It is considered that the alpha particle is preformed on the surface of the emitting nucleus and penetrates the potential barrier [1–4]. Up to now, only few attempts were published that treats the alpha decay within fission models [5–7]. In these recent investigations, it was emphasized that the alpha decay is formed on the surface of the parent in the case of superheavy elements, that the fine structure is due to the Coriolis effect and that the dissipation for superasymmetric fission is much lower than that of the symmetric fission. For the first time, the rearrangement of the single particle levels from the initial ground state of the parent up to the asymptotic configuration were calculated. Fragmentation potentials for all mass asymmetries, including alpha decay were also reported [8–10]

The theoretical study of binary disintegration processes in a wide range of mass asymmetries, including fission and alpha decay, was limited by the difficulties encountered in the calculations of single-particle levels for very deformed one-center potentials. These difficulties were surpassed by considering a mean field generated by nucleons moving in a double center potential. A two-center model allows the description of single-particle energy evolutions from the ground-state up to the formation of two separated fragments [11]. Recently, a Woods-Saxon two center model was developed [12] and its validity for superasymmetric fission processes was tested for cluster decay [13–15], fission [16–22] and even for β -decay [23, 24]. The choice of the ^{240}Pu nucleus was motivated by an intriguing behavior of the relative branch-

ing ratios of the process [25, 26]. A pronounced maximum of the branching ratios for the 4^+ state is an intriguing feature in this region of nuclei.

2. FORMALISM

In the macroscopic-microscopic method, the whole system is characterized by some collective coordinates that approximately determine the behavior of many other intrinsic variables [27–29]. The basic ingredient in such an analysis is the shape parametrization that depends on several macroscopic degrees of freedom. The generalized coordinates associated with these degrees of freedom vary in time leading to a split of the nuclear system into two separate fragments or to the synthesis of the compound nucleus. The macroscopic deformation energy is calculated within the liquid-drop model. A microscopic potential must be constructed in order to be consistent with this nuclear shape parametrization. A microscopic correction is then evaluated using the Strutinsky procedure. We use an axial symmetric nuclear shape that offers the possibility to obtain a continuous transition from one initial nucleus to the separated fragments. This parametrization is obtained by smoothly joining two spheroids of semi-axis a_i and b_i ($i=1,2$) with a neck surface generated by the rotation of a circle of radius R_3 around the axis of symmetry. The distance between the centers of the fragments is denoted R and has the meaning of an elongation. The probability to obtain a binary partition $^{236}\text{U}+\alpha$ is ruled by the barrier penetrability. Using the least action principle, it is possible to obtain the path in the configuration space followed by the fissioning system, and furthermore the associated probability of penetrating the barrier.

In the framework of the cranking model the expression for the momentum of inertia J is [30]

$$J = 2\hbar^2 \sum_{i,j} \frac{\langle \nu | j_x | \mu \rangle^2}{E_\nu + E_\mu} (u_\nu v_\mu - u_\mu v_\nu)^2 \quad (1)$$

where u_ν and v_ν are the vacancy and occupation amplitudes of the level described by the wave function $|\nu\rangle$. The x component of the total angular momentum is

$$j_x = L_x + s_x \quad (2)$$

where

$$\vec{L} = (\vec{r} - \vec{r}_{cm}) \times \vec{p} \quad (3)$$

is the orbital momentum of a particle and s is the spin.

This model can be extended to include statistically the temperature of the system [31].

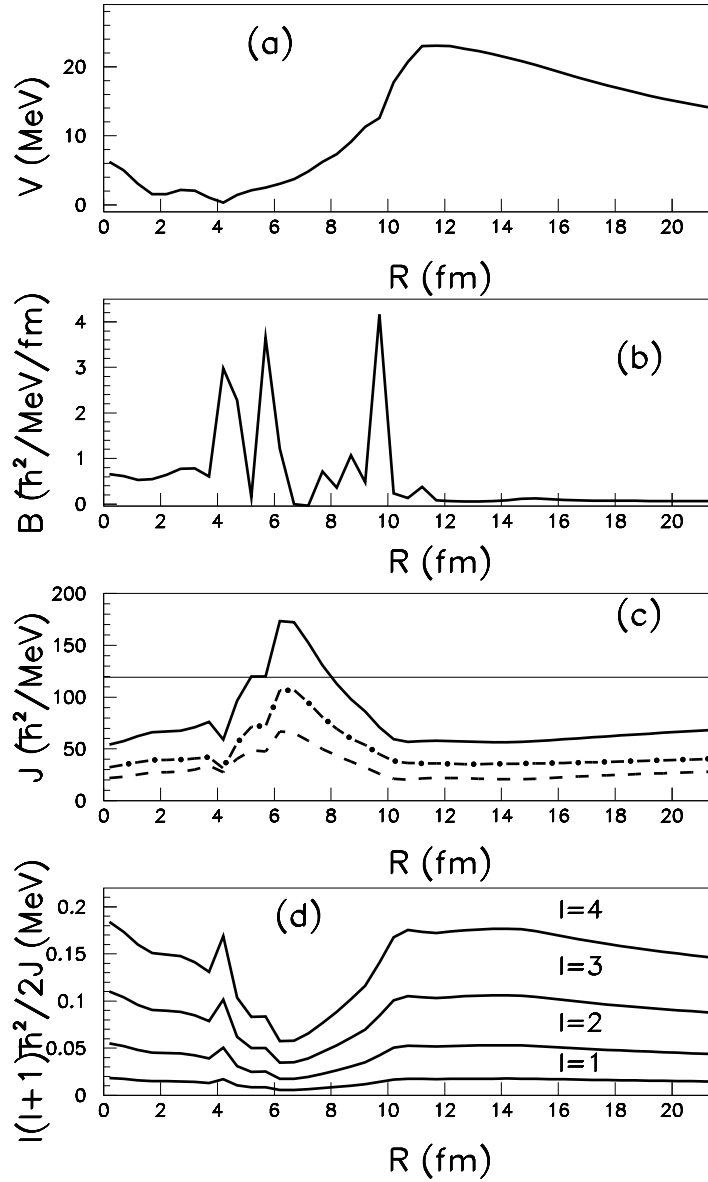


Fig. 1 – (a) The potential barrier V for alpha decay as function of the distance between the centers of the fragments. (b) The effective mass B along the supersymmetric fission trajectory. (c) The moment of inertia J along the alpha decay trajectory. (d) The centrifugal energy for different values of the total angular momentum.

3. RESULTS AND DISCUSSION

The barrier for the α -decay is represented in Fig. 1 (a). The ground state of the ^{240}Pu parent is located in the vicinity of a distance between the centers of the fragments of about 4 fm. Increasing the elongation R , a barrier is formed almost monotonically, without additional minima. That means, no quasistationary states are possible. The effective mass B is displayed in Fig. 1 (b), being computed in the frame of the cranking model [29, 32]. It exhibits a structure along the superasymmetric fission path, with a strong peak close to scission at $R \approx 10$ fm. After $R=10$ fm the system reaches the reduced mass of the $^{236}\text{U}+\alpha$ combination.

The moment of inertia J is plotted in Fig. 1 (c). A thin horizontal line marks the value of the rigid body moment of inertia. As expected, in the ground state configuration, the cranking moment of inertia has a value of $70 \hbar^2/\text{MeV}$, much lower than the rigid body one. After the scission, the moment of inertia increases with a small slope, as expected for two separated bodies. An unexpected fluctuation of the moment of inertia is produced at $R \approx 6$ fm, along the superasymmetric fission trajectory. In order to investigate the influence of this strong variation of the moment of inertia, the centrifugal barrier term $l(l+1)\hbar^2/2J$ is calculated. This term is represented in Fig. 1 (d) for different values of l . The strong fluctuation of the moment of inertia produces a region where the difference between the collective levels associated to rotations are very small. In this region, where the residual interaction between the collective rotational levels is small, it is possible to create a mixing of configuration as those produced by the Landau-Zener effect. Such a promotion mechanism can modify the population of each state during the disintegration.

In conclusion, the level schemes, the potential barrier and the inertia were determined for alpha decay in the framework of the macroscopic-microscopic model. The alpha decay process was treated as a superasymmetric fission process. Moment of inertia were reported for Nilsson two center shell models in the past [33], but it is for the first time that the moment of inertia for alpha-decay is reported. This work is a step towards an unitary treatment of fission, cluster and alpha decay.

Acknowledgements. Work supported by CNCS - UEFISCDI, project number PN - II - ID - PCE - 2011 -3 - 0068.

REFERENCES

1. D.S. Delion, in "Theory of Particles and Cluster Emission", *Lecture Notes in Physics*, volume **819** (Springer, 2010).
2. D.S. Delion, R.J. Liotta, and R. Wyss, *Phys. Rev. C* **76**, 044301 (2007).
3. I. Silisteanu and A.I. Budaca, *Rom. J. Phys.* **58**, 1198 (2013).
4. I. Silisteanu and A.I. Budaca, *Rom. Rep. Phys.* **65**, 757 (2013).

5. A. Sandulescu, M. Mirea, and D.S. Delion, *EPL* **101**, 62001 (2013).
6. M. Mirea, *Phys. Rev. C* **63**, 034603 (2001).
7. N. Shayan Shakib, M. Farhad Rahimi, and M. Mahdi Firoozabadi, *Rom. Rep. Phys.* **65**, 401 (2013).
8. M. Mirea, D.S. Delion, and A. Sandulescu, *EPL* **85**, 12001 (2009).
9. D. Aranghel and A. Sandulescu, *Rom. J. Phys.* **60**, 147 (2015).
10. A. Sandulescu and M. Mirea, *Eur. Phys. J. A* **50**, 110 (2014).
11. J. Maruhn and W. Greiner, *Z. Phys.* **251**, 431 (1972).
12. M. Mirea, *Phys. Rev. C* **78**, 044618 (2008).
13. M. Mirea, A. Sandulescu, and D.S. Delion, *Nucl. Phys. A* **870-871**, 23 (2011).
14. M. Mirea, A. Sandulescu, and D.S. Delion, *Eur. Phys. J. A* **48**, 86 (2012).
15. A. Sandulescu and M. Mirea, *Rom. Rep. Phys.* **65**, 688 (2013).
16. M. Mirea, *Phys. Rev. C* **89**, 034623 (2014).
17. M. Mirea, *Phys. Lett. B* **717**, 252 (2012).
18. M. Mirea, *Phys. Rev. C* **83**, 054608 (2011).
19. M. Mirea, D.S. Delion, and A. Sandulescu, *Phys. Rev. C* **81**, 044317 (2010).
20. M. Mirea, *Phys. Lett. B* **680**, 316 (2009).
21. A.-M. Micu and M. Mirea, *Rom. J. Phys.* **58**, 939 (2013).
22. A. Sandulescu and M. Mirea, *Rom. J. Phys.* **58**, 1148 (2013).
23. T.E. Pahomi, A. Neascu, M. Mirea, and S. Stoica, *Rom. Rep. Phys.* **66**, 370 (2014).
24. S. Stoica and M. Mirea, *Phys. Rev. C* **88**, 037303 (2013).
25. D. Bucurescu and N.V. Zamfir, *Phys. Rev. C* **87**, 054324 (2013).
26. D. Bucurescu and N.V. Zamfir, *Phys. Rev. C* **86**, 067306 (2012).
27. J.R. Nix, *Ann. Rev. Nucl. Sci.* **22**, 65 (1972).
28. W.J. Swiatecki and S. Bjornholm, *Phys. Rep.* **4**, 325 (1972).
29. M. Brack, J. Damgaard, A.S. Jensen, H.C. Pauli, V.M. Strutinsky, and C.Y. Wong, *Rev. Mod. Phys.* **44**, 320 (1972).
30. O. Prior, F. Boehm, and S.G. Nilsson, *Nucl. Phys. A* **110**, 257 (1968).
31. I. Ami, M. Fellah, N.H. Allal, and M.R. Oudih, *Rom. J. Phys.* **59**, 504 (2014).
32. M. Mirea and R.C. Bobulescu, *J. Phys. G* **37**, 055106 (2010).
33. Xizhen Wu, J.A. Maruhn, and W. Greiner, *Z. Phys. A* **334**, 207 (1989).